THE ECONOMIC IMPACT OF A GREAT EARTHQUAKE IN THE CAPITAL REGION OF CHINA

B Shen-Tu[1], M Mahdyiar[1], T Lai[1], K Shabestari[1], and Y Rong[1]

[1] Air Worldwide Corp., Boston, USA
Email: bingming@air-worldwide.com

ABSTRACT: In 1679, Beijing was directly hit by a magnitude 8 earthquake -the Sanhe-Pinggu earthquake, one of the largest historic earthquakes in eastern China. In this study, we investigated the potential economic impact of a similar earthquake hitting the capital region. We developed an earthquake loss estimation model with ground motion intensity calculation and building vulnerability functions specifically calibrated for northeastern China. We use this model to study the effects of rupture scenarios that account for the variation in rupture source parameters and ground motion uncertainties on regional loss distributions. The results show that a repeat of a Sanhe-Pinggu type event near the capital region could cause property damage of over 900 billion Yuan. This is equivalent to about 28% of the total GDP of the five provincial municipalities affected by the event, or 4% the national GDP in 2006.

KEYWORDS: Earthquake Loss, 1679 Sanhe-Pinggu earthquake, China

1. INTRODUCTION

A catastrophic event such as an earthquake or typhoon can disrupt a nation's economic and social activity, change business practices and may even affect government regulations. In 1992, Hurricane Andrew caused11 financial institutions in the United States to become insolvent. This event has changed the way insurance and reinsurance companies assess their business by relying on more quantitative catastrophe (CAT) models. On September 11, 2001, the terrorist attack in New York caused unprecedented economic losses and social impact from a man-made catastrophic event. This event eventually lead several major US airlines into bankruptcy, and triggered a significant economic downturn in the United States, and consequently many other nations..

While natural disasters cannot be avoided, there are ways to minimize losses and impact, increase the awareness of the risks involved. One of the most effective ways to lessen the impact of natural disasters on people and property is through risk assessment and mitigation. A realistic assessment of the vulnerability and potential economic impact from a catastrophic event can help a government prepare for large scale catastrophic events by improving building safety, increasing public awareness, regulate businesses to use proper risk management and transfer tools to minimize loss and avoid an economic downturn.

The main purpose of this study is to assess the scale of direct economic loss due to a potential large earthquake similar to the Sanhe-Pingggu earthquake of 1679 that occurred near Beijing. We assess the economic impact based on property loss. Uncertainty in the estimated loss due to location, source parameter variation, and ground motion uncertainty is evaluated in the context of local geologic and tectonic environment.

An earthquake loss estimation model typically includes the following basic components: a hazard component that defines the seismic source and calculates ground motion (field); an engineering component that estimates vulnerability of various types of structures; an exposure component that establishes the building stock at all sites affected by the event; and an economic component that defines policy terms and risk transfer structures for insured properties (only needed if the interest is on insured loss). HAZUS is one of the earthquake loss estimation models widely used in the United States to estimate scenario losses for future or historic events (e.g. Zoback et al., 2003; NYCEM, 2003). The damage functions in HAZUS are calibrated to the characteristics of US buildings. So are the ground motion calculation equations. Since the predominant building types and vulnerability characteristics in China are quite unique, in order to develop a realistic loss estimation model applicable to China, it is necessary to develop damage functions that are specifically calibrated to characteristics of local buildings. Similarly, the ground motion calculation module should also be tuned to attenuation characteristics of the local crustal or subsurface geological environments. In this study we use an earthquake loss estimation model with all the main components specifically calibrated for China. In the following subsections, we first briefly describe how each of the components is modeled. Then we present the results followed with a discussion on the estimated uncertainty and significance of economic impact.

2. SEISMOTECTONIC SETTINGS AND THE SOURCE PARAMETER OF THE 1679 EARTHQUAKE

2.1 The 1679 Earthquake

The September 2, 1679, earthquake occurred in Pinggu county of the Beijing municipality, and the Sanhe county of Hebei province, about 40 km east of Beijing. The magnitude of this event is estimated at 8 from intensity data (GU, 1983). It is the largest known historic earthquake near Beijing. This event flattened several towns and villages in the epicentral area and killed more than 45,000 people. Historic records (annals) from 165 counties documented this event, indicating that it impacted an area of over 10,000 square km. Many structures in the Forbidden City in central Beijing, about 50 km from the epicenter, suffered severe damage.

This earthquake occurred along the Xiadianxing or Mafang-Xiadian fault, a hidden fault mostly buried under loose Quaternary sediment (Figure 1). Except for the 10 km surface break created by the earthquake, the Mafang-Xiadian fault cannot be traced at the surface; it is only inferable from subsurface geological (drilling) and geophysical (seismic survey) data (Xu et al., 2002). The total length of the Mafang-Xiadian fault is about 120 km and its slip rate is inferred to be 0.45 mm/yr (Xu et al., 2002). Because of the slow deformation rate, the probability of such a large earthquake to reoccur along this same fault in the near future should be very low. However, the active tectonic zone – the North China seismic belt where the Mafang-Xiadian fault and Beijing are located –has a series of active faults similar to the Mafang-Xiadian fault that could be the source of potential large earthquakes (Figure 1). The Tangshan fault is another active fault about 100 km east of the Mafang-Xiadian fault in this seismic belt that generated the Ms 7.8 Tangshan earthquake in 1976. Hence the threat from such an earthquake is not unrealistic. The regional tectonics and historic seismicity described in the next section may further demonstrate this potential.

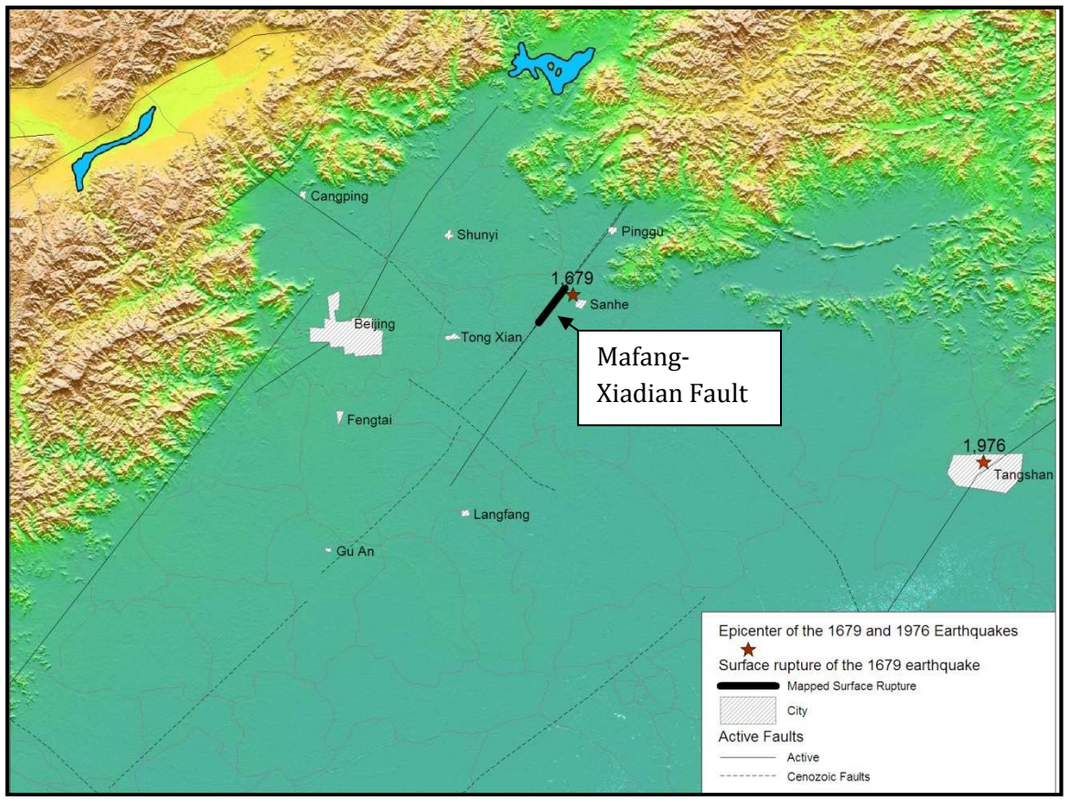

Figure 1 Epicenter and surface rupture of the 1679 earthquake and local active strucutres

2.2 *Tectonic Settings*

Beijing is located within the north China tectonic province (tectonic block), which is the northern part of the Amur plate. As a tectonic plate, the Amur plate is considered to be relatively rigid (Heki et al., 1999). However there is significant internal deformation within the Amur plate, especially within the north China tectonic province, as evidenced by the repeat occurrence of large to great historic earthquakes and the development of graben-horst or basin-range structure in the region in Cenozoic time. Several distinctive active fault belts exist within this North China tectonic province that has hosted all the major historic seismic activity: the active fault belt surrounding the Ordos fault block in the west, the Tan-Lu fault system in the east, and the North China plain between the Tan-Lu fault system and Taihang-Wutai Mountain fault block (Figure 2).

The Ordos fault block is a relatively rigid block that experiencing little deformation in the Cenozoic time. It is surrounded by a series of fault-bounded basins on the north (the Hetao-Linhe fault basin), the south (the Weihe fault

Basin), and the east (the Shanxi rift system). The 1303 Hongtong and 1556 Huaxian earthquakes, both of magnitude 8, all occurred in this seismic belt.

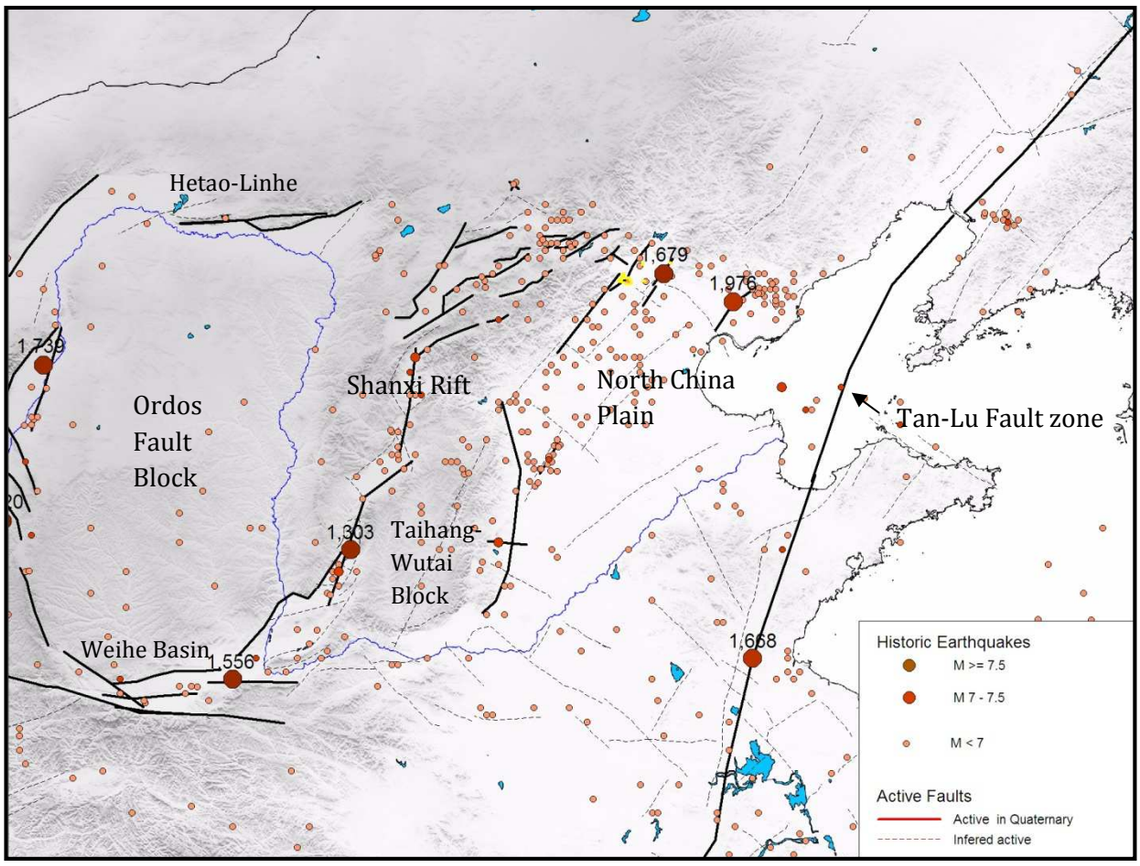

Figure 2 Regional tectonic setting of Beijing – the North China tectonic province.

The Tan-Lu fault zone is the largest active fault system in eastern China. It is a right-lateral fault system with slip rates of 1-3 mm/yr in late Quaternary (Deng, 2003). The 1668 M8.5 earthquake occurred along this fault.

The North China plain is composed of a series of Cenozoic basin and range or horsts and grabens separated by normal faults. Most of these horst and graben structures were formed in the Paleogene time. During the Neogence and Quaternary periods the region subsided as a whole, with thick deposits covering the horst-graben structure, eliminating any surface expression. As a result, most of the seismogenic faults are buried or hidden under the thick Quaternary cover. Recent seismic activity such as the 1679 M8 and 1976 M7.5 Tangshan earthquakes all occurred on faults that along the Cenozoic basins and are a result of the reactivity of these existing Cenozoic faults under NEE – SWW compressive regional stress field (Xu et al., 1992).

2.3. Source Parameters of the 1679 Event

The September 2, 1679, earthquake occurred about 40 km east of Beijing along the Xiadianxing or Mafang-Xiadian fault. This fault is oriented about N50E with a high dip angle of 50°-70°, dipping southeastward (Figure 1). The thickness of Quaternary deposits on the two sides of the fault differ by about 200 to 400 meters, suggesting that this fault may have been active in the Quaternary time with a significant dip-slip component. However there is no surface expression for this fault other than a 10 km long surface break caused by the 1679 earthquake (Xiang et al., 1988). The 10 km coseismic rupture at the ground is probably not representative of the seismic source for the event. Worldwide statistical data show that a magnitude 8 earthquake should have a length of about130 km for normal faulting events, or 245 km for strike-slip faulting events (Wells & Coppersmith, 1992). The short length of the coseismic break at the surface indicates that only a small portion of the coseismic rupture broke the surface. The main part of coseismic rupture is buried under the loose deposits and did not reach to the ground. Due to the hidden nature of this seismogenic fault, the source parameters for this earthquake are therefore quite uncertain. The main uncertainty probably lies in the rupture length and magnitude, and as stated earlier, the length of surface rupture probably significantly underestimates the rupture dimension of the event. However, the total length of the source fault is about 100 to 120 km (Xu et al., 2002; Gao et al., 1993). Therefore a possible length of the rupture should be larger than 10 km but less than 120 km. Given the size of the earthquake, the length would most likely exceed 50 km. We use three lengths - 60 km, 90 km, and 120 km, to represent the range of rupture length for this event. The

60 km length represents the northern segment of the Mafang-Xiadian fault. This segment extends from north of Pinggu in the northeast to south of Tongxian for about 60 km where it intercepts with a NW-SE striking fault (Figure 1). The southward extension of this fault is debatable and there could be an offset between this segment and the segment further to the southwest. This segment also crosses the three counties in the epicentral area that had the heaviest damage in 1679. The 120 km length represents the maximum extension of this seismogenic fault and the 90 km length is an intermediate value between the two.

The magnitude of this event was estimated based on seismic intensity inferred from historic records. There is a great deal of uncertainty in estimating pre-instrumental earthquake magnitude because of the semi-quantitative nature of seismic intensity, and the subjectivity in assigning a seismic intensity based on descriptions in damage or felt reports. This event occurred about 100 km west of the 1976 Mw 7.5 Tangshan earthquake. Both this event and the 1976 Tangshan earthquake occurred in the same tectonic province with similar geological and tectonic environments. The 1976 Tangshan earthquake generated an 8-km long surface rupture, and the total rupture length of Tangshan earthquake is estimated to range from 48 km to 100 km (Xie & Yao, 1991; Kanamori & Allen, 1986; Huang & Yeh, 1997). The scale of the rupture from the 1679 earthquake is slightly larger than that of the 1976 earthquake both in terms of source length and surface rupture, indicating that the 1679 event could have a larger total coseismic slip. Given that the total length of the Mafang-Xiadian fault is comparable to the Tangshan fault responsible for the 1976 earthquake, if we assume that the average coseismic slip of the 1679 earthquake is twice the maximum coseismic slip (4.5 m) of the Tangshan earthquake obtained by different studies (Xie & Yao, 1991; Huang & Yeh, 1997), the magnitude of the 1679 could be as low as 7.67. We assume that this is the lower limit for the magnitude of the 1679 earthquake. For the upper bound limit, we use 8.0, which is also the upper bound magnitude for the entire North China tectonic province recommended in various studies (Xu et al., 2002). Table 1 summarizes the range of source parameters that we use for loss calculation purposes.

Table 1 Source parameter variation for the 1679 Sanhe-Pinggu earthquake

Parameter	Range
Length(m)	50, 90, 120
Width(m)	20, 25
Magnitude(Mw)	7.6, 7.8, 8.0
Dip	78

3. GROUND MOTION

Because there are very limited strong motion data available in China, empirical ground motion attenuation relationships developed based on local strong motion data are not available for this region. However a great deal of historic intensity data (maps) have been published and used to develop empirical intensity attenuation functions (State Seismological Bureau of China, 1990). Several recent studies (e.g. Hu & Zhang, 1984; Huo & Hu (1992) have used intensity data in China combined with strong motion data in the western US and China to develop attenuation equations for four different regions of China. The 2001 national seismic hazard map of China took a such an approach to develop region-dependent attenuation functions for the probabilistic hazard calculations. Huo & Hu (1992)'s result shows that attenuation is faster in southwest and southeast China than in northwest and northeast China. This difference is mainly influenced by differences in intensity attenuation relations in the four regions.

Since our loss calculation model use spectra accelerations, whereas Huo & Hu (1992) have only provided PGA attenuation functions, we used a slightly different approach to calculate the ground motion for this event. A comparison of Huo & Hu's attenuation relations with the attenuation equations for western US (WUS) recommended by USGS (Frankel et al., 1996) shows that, for earthquakes whose magnitudes are larger than 6.5, Huo & Hu's attenuation equation for northeast China gives consistently higher PGA than the WUS attenuation equations at distances of under100 km. A weighted combination of WUS and central and eastern US (CEUS) attenuation functions used by the USGS can provide a good match to the result of Huo and Hu as well as the available strong motion data. The weighting factors that best match Huo and Hu's results would need to be magnitude-dependent. For events with magnitudes larger than 7, an equal weighting for the two sets of attenuation equations of WUS and CEUS provide reasonable matches to the observed data from the 1976 Tangshan earthquake and the results of Huo and Hu (1992) (Figure 3). We calculated seismic intensity from the calculated ground motions using the conversion equations of Kaka and Atkinson (2004) for comparison with the observed intensity field of historic earthquakes as a calibration process for determining the weighting factors. For the few significant

historic earthquakes in north China, the modeled intensity fields match the observed intensity fields reasonably well.

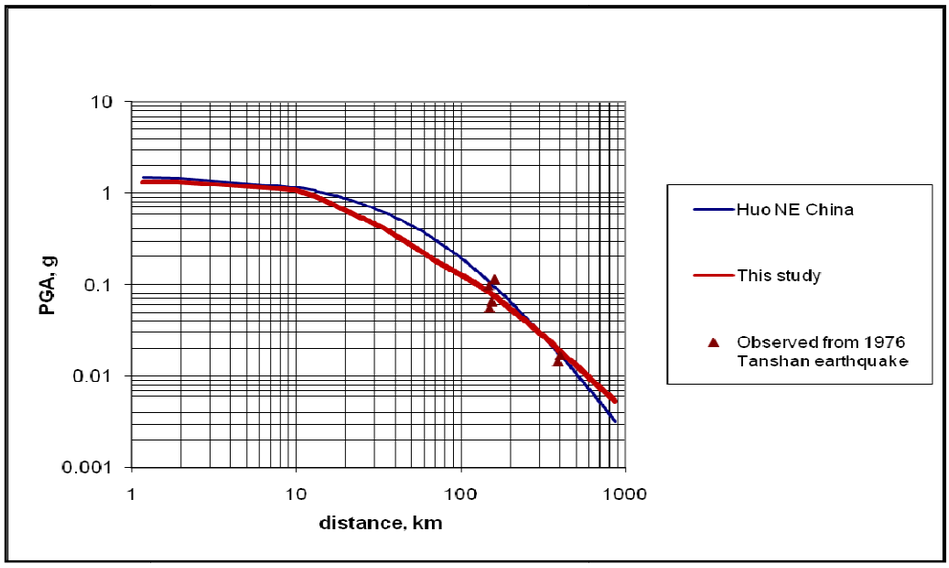

Figure 3 Comparison of ground motion (PGA) predicted by Huo & Hu (1992, thin blue line), this study (thick red line), and observed during the 1976 Tangshan earthquake (triangles)

Site effect is considered in the ground motion calculation. Each site is classified into the extended NEHRP soil types based on surface geological information, and amplification is calculated using the average 30-meter shear wave velocity for each class type (Wills et al., 2000).

The uncertainty associated with ground motion could significantly affect the calculated loss. Most recent empirical attenuation equations formulate the ground motion uncertainties into inter- and intra-event components. The inter-event component reflects uncertainties in the seismic source (stress drop, slip distribution, rupture direction etc.). Intra-event uncertainty reflects the combined path, site, and other non-source related effects (Abrahamson and Silva, 1997; Lee & Anderson, 2000). Intra-event uncertainty is relatively more complex and it is generally difficult to decouple the effects of intra-event ground motion uncertainty from variations in building vulnerability. In order to provide a sense of uncertainty in the estimated loss due to ground motion uncertainty, we used the uncertainty parameters estimated by empirical ground motion attenuation equations. For simplicity, we limited our analysis to inter-event uncertainty and assumed that any bias due to intra-event uncertainty is partially captured in the process of calibrating the damage functions. To account for the inter-event uncertainty, we simulated ground motion fields hundreds of times for each source scenario by adding a random uncertainty within the range of ± 2 sigmas. Uncertainty in the estimated loss is then calculated from the variations in the estimated loss from all the runs.

4. DAMAGE ESTIMATION

Earthquake-induced building damage is caused by the building's dynamic response to ground motion, which can vary substantially depending on characteristics of both the ground motion and the building. Building response ,and its associated damage status to earthquake shaking, are complex phenomena. It is believed that the damage could be best measured by deformation. For this reason our vulnerability module adopted the capacity spectral method to estimate building deformation subjected to earthquake ground motion.

The development of building capacity curves is quite comprehensive. It was derived from the building's period, deformation capacity and ductility, yield, and ultimate strength. These physical parameters are based on experimental observations, published analytical research, design standard, and published empirical relations. For modern engineered structures, these parameters are tuned to be compatible with the general objective of China building codes (GB 50011 - 2001), i.e., "no damage for frequent levels of shaking, damage repairable for occasional levels of shaking, and collapse prevention for rare levels of shaking." The "frequent," "occasional" and "rare" shaking level are quantitatively defined in terms of PGA values in the building code. The capacity of a building to resist the lateral force imposed by an earthquake is represented by a force-displacement curve (the building's capacity curve). The building's important seismic characteristics, such as material brittleness and ductility, are reflected in its capacity curve. The demand imposed by an earthquake on a building is represented by the response spectrum curve. When these two curves are plotted on the spectral acceleration (S_a) vs. spectral

displacement (S_d) plane, their intersection corresponds approximately to the maximum displacement of the building in response to the ground motion (Figure 4).

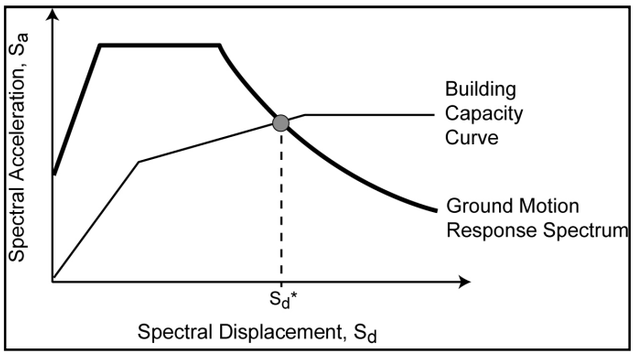

Figure 4 Capacity Spectrum Method

The development of deformation-based damage functions is relatively easy and straightforward. The relation between building deformation and damage is well documented in literature. For the several common type of buildings in China (confined masonry, unreinforced masonry, and mid to low-rise reinforced concrete buildings), we have used data from several historic earthquakes (such as the 1978 Tangshan, 1992 Lijian earthquakes etc) to calibrate our damage functions. For modern engineered structures, especially those mid to high- rise RC and steel buildings, we rely on historic data from recent significant earthquakes in other regions such as Taiwan (the 1999 Ji-Ji earthquake) and Japan (the 1995 Kobe earthquake), combined with published experimental studies to develop our damage functions. There is a total of 27 basic damage functions for 27 different type of structures representative in the Chinese building inventories.

The mean damage values of the basic damage functions are further adjusted to account for building age, region variations in design and construction practice, etc. The final damage functions are calibrated using damage data from significant historic earthquakes that have occurred in the last 50 years in China.

5. EXPOSURE

Before one can estimate the potential loss of an earthquake, we must first know the total value of the building stock exposed to the earthquake. In order to make a realistic estimation, we must also know the type of the building and its spatial distribution.

Beijing is the political, cultural and economic center of China. As China experienced double-digit increases in economic growth over the past few decades, Beijing's building inventory has also grown rapidly. According to the National Bureau of Statistics (NBS) (2007), the total residential living space in the urban districts of Beijing increased from 152 million square meters at the end of 2000, to 310 million square meters at the end of 2006. It has therefore more than doubled over a period of 6 years. The average construction cost also increased significantly during the same time period, with the average cost for buildings constructed by real estate developers reaching 2000-2400 Yuan for each square meter of construction area. Thus in the urban district alone, Beijing's residential property replacement value has exceed 600 billion (RMB) Yuan in 2006.

In this study, we use AIR Worldwide Corporation's 2007 industry exposure database for China to estimate the potential property loss for this event. This exposure database is based on the 2000 and 2001 residential and commercial census data as well as yearly statistical data on construction, real estate, fixed asset investment and other construction and city development information from 2000 to 2007. The primary sources of the data include the National Bureau of Statistics and the Ministry of Construction of China, the provincial bureaus of statistics (e.g., the Beijing Municipal Bureau of Statistics), and the China Index Academy. The census data are at county/Qu level containing detailed information on residential living area, housing type (by wall material), age, and building height (number of stories). The database used detailed information on construction areas of various types of buildings (e.g., residential, commercial etc.), average construction costs of different type of buildings, building height, wall material, and building age, as well as information on population, family unit counts, number of employees and establishments in various business categories, to estimate the replacement value of the predominate types of buildings in each municipality (county/Qu). The buildings in the database are classified according to ground motion

vulnerability sensitive parameters such as structure type (e.g., unreinforced masonry, confined masonry, reinforced concrete, steel frame etc.), height, age, and occupancy. Since the main data are at the county/Qu level, the exposure is first estimated for each county level municipality. The county level exposure is then distributed to a 5 km by 5 km grid based on population density within the county. Table 2 lists the total replacement values (including structures and contents) for residential, commercial, and CAR/EAR (properties under construction) in the five municipalities/provinces (Beijing, Tianjin, Hebei, Shanxi, and Inner Mongolia) in and around the capital region. The total exposure in the five provincial municipalities is estimated to be about 7.48 trillion (RMB) Yuan or 1 trillion US dollars.

Table 2 Total exposure in Beijing, Tianjin, Hebei, Shanxi, and Inner Mongolia

Total Exposure	Residential	Commercial	CAR/EAR
(Billion Yuan)	2,387	4,448	650

Masonry (unreinforced or confined masonry) is a popular construction type in this region, especially in rural areas and in buildings constructed a few decades ago. According to NBS (2007), over 80% of the current residential houses in rural regions are masonry. The AIR exposure database shows that about 60% of the total exposure in the five provincial municipalities are masonry buildings; the remaining ones are predominately reinforced concrete. Of the 60% masonry buildings, about one third is unreinforced masonry, which is extremely vulnerable to seismic hazard.

6. RESULT AND DISCUSSION

The various combinations of magnitude, rupture length, and width listed in Table 1 come to 18 different source scenarios. The average total loss of the 18 scenarios is 846 billion RMB Yuan (about 120 billion USD) with one standard deviation of about 130 billion RMB (about 18 billion USD). To account for the uncertainties associated with ground motion, we ran 500 times for each of the source scenarios with a random uncertainty (in the range of ± 2 sigma) added to the mean ground motion. The average loss of all the scenarios was then 935 billion Yuan, with one standard deviation of 520 billion Yuan. Both the mean loss and standard deviation increased after accounting for the uncertainty in ground motion, which is expected due to the non-linear relationship between the ground motion and the damage ratio. The total affected exposure is about 5 trillion Yuan. Hence the average loss represents about 18.7% of the total affected exposure (mean damage ratio).

The earthquake would impact 160 to 175 counties in seven provinces: Beijing, Tianjin, Hebei, Shanxi, Neimeng (Inner Mongolia), Liaoning, and Shandong, over a radius of 220 km to 280 km (Figure 5). This is consistent with historic records, which indicate damage observed as far south as the Shandong province, and north to Neimeng (Inner Mongolia), covering an area of 10,000 square km. The main damage (over 99%) however fall within the Beijing and Tianjin municipalities and the Hebei province, with 75 to 80% of the total losses occurring in the Beijing municipality. The heavy losses in Beijing is mainly due to its close proximity to the earthquake source and its high concentration of exposure (Beijing accounts for 50% of the total exposure of the three municipalities). The mean damage ratio for the Beijing municipality is about 30%. Losses from residential properties account for less than 1/3. The main loss is due to damage to commercial and industrial properties (Table 3).

Table 3. Average total loss (billion Yuan) by exposure type

Residential	Commercial	CAR/EAR	Total
291	632	12	935 ±520

The size of this earthquake is about the same as the May 12, 2008, Wenchuan earthquake in the Sichuan province, which caused tremendous disturbance in the social and economic activity in Sichuan, as well as in the entire country of China. Estimated direct losses for this event reported in the media are mostly under 200 billion Yuan. Our estimated loss for this event is 4-5 times larger than the estimated loss from the Wenchuan earthquake. The average total loss represents 28% of the total GDP of the Beijing, Tianjin, Hebei, Shanxi, and Neimeng provinces in 2006 (NBS, 2007). If we further consider losses due to business interruption and damage to infrastructure, the total direct loss could easily exceed 1 trillion Yuan (140 billion USD) or more than 30% of the regional GDP in the five provinces. Considering the fact that the affected area is the political, social, and economic center of China, the economic and social impact of such a event could be much larger than that caused by the Wenchuan earthquakes.

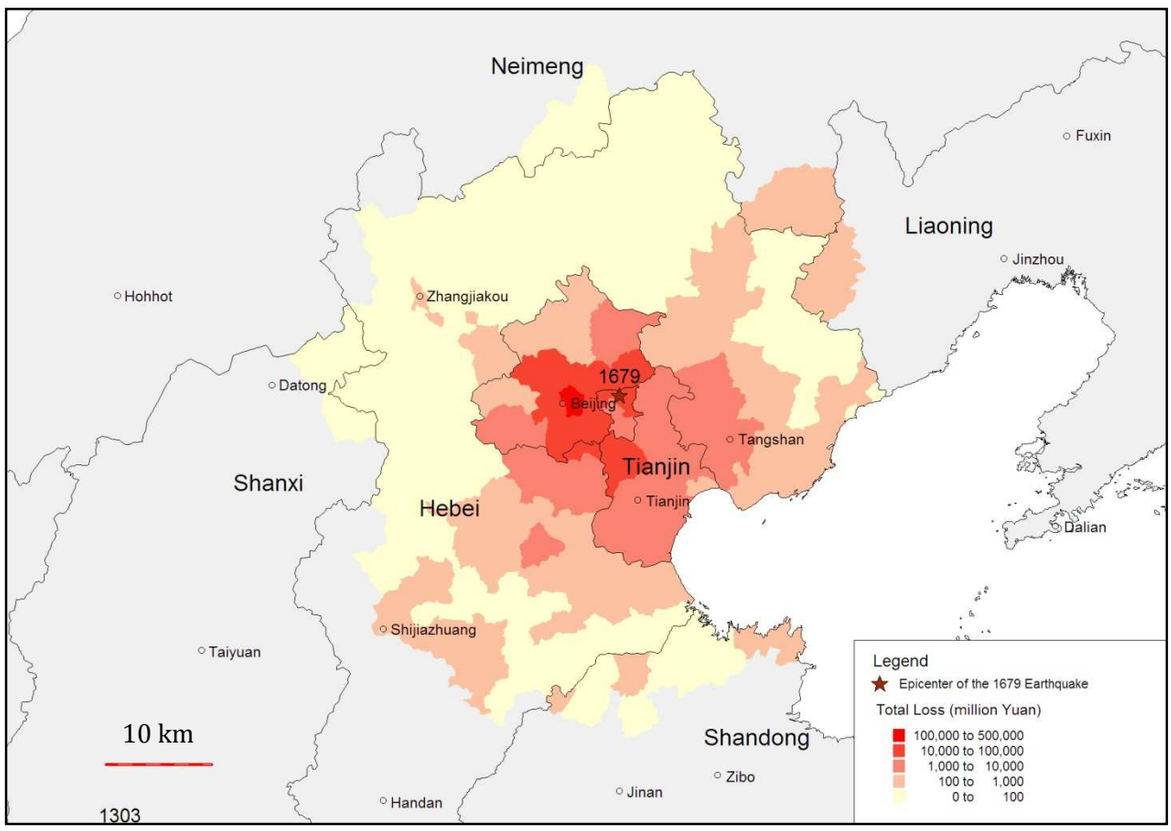

Figure 5 Distribution of estimated total loss by county from one earthquake scenario

REFERENCE

Abrahamson, N.A., W.J. Silva (1997), Equations for estimating horizontal response spectra and peak acceleration from western north America earthquakes: A summary of recent work, *Seism. Res. Lett.* 68:1, 94-1217.

Deng, Q., P. Zhang, Y. Ran, X. Yang, M. Wei, Q Chu (2003), Basic characteristics of active tectonics of China, *Science in China, 46:4*, 356-372.

Frankel, A., Mueller, C., Barnhard, T., Perkins, D., Leyendecker, E. V., Dickman, N., Hanson, S., and Hopper, M. (1996). National Seismic-Hazard Maps: Documentation June 1996, *United States Geological Survey Open-File Report 96-532*.

Gao, W. and J. Ma (Chief editors)(1993), Earthquake Geological Environment and Earthquake Hazard in the Capital Region, Seismological Press, Beijing.

Gu, Gongxu (Chief editor) and 8 others (1983), Catalog of Chinese earthquakes (1831 B.C. – 1969 A.D.), Science Press, Beijing.

Heki, K., S. Miyazaki, H. Takahashi, M. Kasahara, F. Kimata, S. Miura, N. F. Vasilenko, A. Ivashchenko, and K. An (1999), The Amurian Plate motion and current plate kinematics in eastern Asia, *J. Geophys. Res.* ***104:*** *B12*, 29147–29155.

Huang, B.-S., and Y.T. Yeh (1997), The fault ruptures of the 1976 Tangshan earthquake sequence inferred from coseismic crustal deformation, *Bull. Seismol. Soc. Am., 87:4*, 1046-1057.

Hu Y. and M Zhang (1984), Method of estimating strong ground motion parameters in the regions lacking ground motion recording, *Earthquake Eng. Eng. Vibration 4:1*, 44-53.

Huo, J. and Y. Hu (1992), Study on attenuation laws of ground motion parameters, Earthquake Engineering and Engineering *Vibration 12: 3*, 1-14 .

Kaka, S.I., and G.M. Atkinson, Relationships between instrumental ground-motion parameters and modified Mercalli intensity in eastern North America, *Bull. Seism. Soc. Am. 94:5*, 1728-1736

Kanamori, H. and C. R. Allen (1986). Earthquake repeat time and average stress drop, in Earthquake Source Mechanics, S. Das, J. Boatwright, and C. H. Scholz. (Editors), *American Geophysical Monograph 37*, 227-235.

Lee, Y., J.G. Anderson, and Y. Zeng (2000). Evaluation of empirical ground motion relations in southern California, *Bull. Seism. Soc. Am. 90: 1*, 136-148.

National Bureau of Statistics of China (2007), China Statistic Year Book, China Statistics Press, Beijing.

New York City Area Consortium for Earthquake Loss Mitigation (NYCEM) (2003), Earthquake risks and mitigation in the New York, New Jersey, and Connecticut region, *Monograph*, www.nycem.org.

State Seismological Bureau of China (1991), Seismic Zonation Map of China, Seismological Press, Beijing.

Wells, D.L. and K.J. Coppersmith (1994), New Empirical relationships among magnitude, rupture length, rupture width, rupture area, and surface displacement, *Bull. Seism. Soc. Am. 84:4*, 974-1002.

Wills, C.J., M. Petersen, W.A. Bryant, M. Reichle, G.J. Saucedo, S.Tan, G. Taylor, and J. Treiman 2000, A site-conditions map for California based on geology and shear-wave velocity, *Bull. Seism. Soc. Am. 90:1*, 187-208.

Xiang, H., Z Fang, J Xu, and others (1988), Study on the tectonic setting and recurrence intervals of large earthquakes in the seismic source zone of the 1679 magnitude Sanhe-Pinggu earthquake, *Earthquake Geology 10:1*, 15-28.

Xie, X. and Z. Yao (1991). The faulting process of Tangshan earthquake inverted simultaneously from the teleseismic waveforms and geodesic deformation data, *Phys. Earth Planet. Interiors 66*, 265-277.

Xu, XW, WM Wu, XK Zhang, SL Ma, WT Ma, GH Yu, ML Gu, WL Jiang (2002), Active Tectonics and Seismicity in the Latest Geological Time in the Capital region of China, Science Press, Beijing (in Chinese).

Zoback, M.L., J. Fenton, K. Miller, C. Wills, B. Rowshandel, and J. Perkins (2003), Earthquake Loss Estimates for the San Francisco Bay Area: the ten most likely events in the next thirty, *3rd Disaster Resistant California Conference, April 22-24, 2003, San Jose, California.*